

Short-range ordering and equilibrium structure of binary crystal mixtures of atomic nuclei in white dwarf cores

D. A. Baiko

Ioffe Institute, Politekhnikeskaya 26, 194021 Saint Petersburg, Russia

(Dated: April 17, 2025)

Mixtures of bare atomic nuclei on a nearly uniform degenerate electron background are a realistic model of matter in the interior of white dwarfs. Despite tremendous progress in understanding their phase diagrams achieved mainly via first-principle simulations, structural, thermodynamic, and kinetic properties of such mixtures are poorly understood. We develop a semi-analytic model of the crystal state of binary mixtures based on the concept of mutual short-range ordering of ions of different sorts. We derive analytic formulas for electrostatic energy of crystal mixtures, including the effect of static ion displacements from the lattice nodes, and estimate their residual entropy. Then we perform free energy minimization with respect to the order parameters for a C/O mixture at all relevant compositions and temperatures. The resulting C/O phase diagram is in a reasonable agreement with that obtained in the most recent first-principle study. The equilibrium microstructure of a crystallized mixture is shown to evolve with decrease of temperature which, in principle, can induce structural transitions. The latter will be accompanied by thermal energy release. The proposed theory opens up a path to analyze ordering and construct phase diagrams of ternary mixtures, which are of great practical interest in astrophysics, as well as to improve calculations of electron-ion scattering rates and kinetic properties of dense crystallized matter.

Introduction – Matter in the inner layers of white dwarfs (WD) and in the outer neutron star crust is compressed by immense gravity of these objects to densities which may be as high as $\sim 10^{10}$ - 10^{11} g/cm³. The result is a complete stripping of electrons off the atomic nuclei and a formation of ion plasma with a nearly uniform background of degenerate electrons. The temperature of matter quickly drops below typical ion interaction energies and the ions condense into a strongly coupled liquid which later freezes into a solid. In principle, nuclei of several different sorts may be present simultaneously at a given density. Physical properties of such ion mixtures are important for various applications, particularly, for stellar evolution modeling. For instance, it has been shown recently that ²²Ne distillation controlled by the phase diagram of a crystallizing ternary ion mixture may cause multi-billion year cooling delays of WD [1–3].

Understanding phase diagrams of ion mixtures has been steadily improving thanks to impressive research over the past several decades [4–12]. The decisive progress has finally been achieved through advanced first-principle simulations [2, 13–21]. While simulations of classic liquid mixtures, especially at moderate couplings, are seemingly straightforward, this is not so for the crystal state where there are mutually conflicting requirements. One needs higher N to be closer to the thermodynamic limit but, on the other hand, crystal simulations tend to stick to an initial ion arrangement and thus one has to explicitly explore ion permutations, possible number of which rapidly grows with N . As a result, the actual structure of multicomponent crystal mixtures is currently unknown to the point that it is unclear whether placement of different ions onto lattice nodes should be treated as random or not.

In this work, we investigate, for the first time, the microstructure of binary crystal mixtures of atomic nuclei.

We do that semi-analytically by introducing order parameters, describing average relative positions of ions of two sorts in a lattice, by expressing electrostatic energy and residual entropy via these parameters, and by minimizing free energy with respect to them. In this way, we establish that the crystal mixture is not fully disordered but prefers a short-range order which, under the assumption of thermal equilibrium, evolves with temperature decrease.

Order parameters and electrostatic energy – Suppose that we have a binary mixture of ions with charge numbers Z_1 and Z_2 , $Z_1 < Z_2$, and charge-neutralizing rigid background of electrons with density n_e . Let the number fraction of Z_2 ions be x . The average ion charge number is then $\langle Z \rangle = xZ_2 + (1-x)Z_1$. Suppose that the ions are arranged in an ideal crystal lattice, one of the nodes of which is chosen as the origin while all the others are specified by lattice vectors \mathbf{R} . The number density of the lattice nodes is $n_i = n_e/\langle Z \rangle$. If the lattice is assumed to be of the bcc type, its spacing $a_1 = (2/n_i)^{1/3}$.

The structure of the mixture is fully determined by specifying the function $Z(\mathbf{R})$ which can take values Z_1 and Z_2 . Let us decompose this function as $Z(\mathbf{R}) = \langle Z \rangle + \delta Z(\mathbf{R}) = \langle Z \rangle + Z^+ \Delta^+(\mathbf{R}) - Z^- \Delta^-(\mathbf{R})$, where $\Delta^+(\mathbf{R}) = 1$ for nodes occupied by Z_2 -ions and 0 otherwise, $\Delta^-(\mathbf{R}) = 1 - \Delta^+(\mathbf{R})$ (see also [22]).

Let us consider the expression

$$P^+(\mathbf{R}) = \frac{1}{N} \sum_{\mathbf{R}_1} \Delta^+(\mathbf{R}_1) \Delta^+(\mathbf{R}_1 + \mathbf{R}), \quad (1)$$

where N is the total number of ions and thermodynamic limit is understood. $P^+(0) = x$. If lattice vectors \mathbf{R}_{1n} and \mathbf{R}_{2n} point to a nearest neighbor and to a next nearest neighbor, which are always occupied, say, by a different ion and by an ion of the same sort, respectively, then $P^+(\mathbf{R}_{1n}) = 0$ and $P^+(\mathbf{R}_{2n}) = x$. If, at large

\mathbf{R} , the mutual placement of ions becomes independent, $P^+(\mathbf{R} \rightarrow \infty) \rightarrow x^2$. If the limit is different from x^2 or if there is no limit at all (e.g. in a perfectly ordered CsCl crystal at $x = 1/2$, P^+ oscillates between 0 and $1/2$), there is a long-range order.

In this work, we shall assume that there is no long-range order (but see [23]). At finite arguments, $P^+(\mathbf{R}_{in})$ is isotropic, i.e. the same for all neighbors of the same order, and we denote it as α_i , the i th short-range order parameter. We emphasize that the definition (1) implies averaging over \mathbf{R}_1 , which means that the actual composition in the vicinity of any particular ion can be essentially arbitrary. The concept of short-range and long-range order is not new: see, e.g., [24] and references therein. However, it has never been applied to dense mixtures of bare atomic nuclei. Our definition of α_i is slightly different from that of [24].

In Table I, we collect several parameters for the first 8 shells of nearest neighbors in the bcc lattice. In particular, we show cartesian coordinates of a vector, belonging to each shell, from which coordinates of all the other equivalent vectors can be obtained by symmetry transformations (arbitrary combinations of coordinate permutations and sign changes), the vector length, l , the total number of neighbors in the i th shell, m_i .

Expanding $\Delta^+(\mathbf{R})$ in the Fourier-integral

$$\Delta^+(\mathbf{R}) = \int_{\mathbf{B}_1} \frac{d\mathbf{k}}{(2\pi)^3 n_i} [x(2\pi)^3 n_i \delta(\mathbf{k}) + \Delta_{\mathbf{k}}^+] e^{i\mathbf{k}\mathbf{R}}, \quad (2)$$

where $\Delta_{\mathbf{k}}^+$ is regular and \mathbf{k} is any vector in the first Brillouin zone, \mathbf{B}_1 , one can deduce that

$$\frac{1}{N} |\Delta_{\mathbf{k}}^+|^2 = x(1-x) + \sum_{i=1}^{\infty} (\alpha_i - x^2) \sum_{\mathbf{R}_{in}} \cos(\mathbf{k}\mathbf{R}_{in}). \quad (3)$$

Naturally, the left-hand side of equation (3) must be non-negative at all \mathbf{k} which restricts allowed values of α_i .

On average for a Z_2 -ion, $m_i \alpha_i / x$ neighbors of the i th order are also Z_2 -ions, whereas for a Z_1 -ion, $m_i(1-2x + \alpha_i)/(1-x)$ neighbors of the i th order are Z_1 -ions. The total number of these ions should be non-negative and $\leq m_i$ as well as the same for a short-range ordered and for a completely disordered system. This produces further constraints: $\max(0, 2x-1) \leq \alpha_i \leq x$ and

$$\sum_i m_i (\alpha_i - x^2) = 0. \quad (4)$$

With these definitions, the electrostatic energy per ion, assuming that all ions are situated exactly at their lattice nodes, can be written as

$$U = \langle U \rangle + U_{\text{corr}} = -\zeta \frac{\langle Z \rangle^2 e^2}{a_i} + \frac{e^2}{2N} \sum'_{\mathbf{R}, \mathbf{R}_1} \frac{\delta Z(\mathbf{R}) \delta Z(\mathbf{R}_1)}{|\mathbf{R} - \mathbf{R}_1|},$$

where ζ is the Madelung constant and $a_i = (4\pi n_i/3)^{-1/3}$. Note that $\langle U \rangle$ is different from the standard linear mixing formula (e.g., [4]), which contains $\langle Z^{5/3} \rangle$ instead.

i	\mathbf{R}_{in}	$4l^2/a_i^2$	m_i	$a_i T_i$	$a_i(I_i - T_i)$
1	$a_1(1/2, 1/2, 1/2)$	3	8	4.4334	0.1149
2	$a_1(1, 0, 0)$	4	6	3.0577	-0.1035
3	$a_1(1, 1, 0)$	8	12	4.1411	0.0368
4	$a_1(3/2, 1/2, 1/2)$	11	24	7.2268	-0.1009
5	$a_1(1, 1, 1)$	12	8	2.1968	0.0774
6	$a_1(2, 0, 0)$	16	6	1.4950	-0.0179
7	$a_1(3/2, 3/2, 1/2)$	19	24	5.3710	0.0510
8	$a_1(2, 1, 0)$	20	24	5.2993	-0.0146
0				0.90183	

TABLE I: Neighbors of the first 8 orders and numerical values of T_i and $I_i - T_i$

The second term reduces to

$$U_{\text{corr}} = \frac{(Z_2 - Z_1)^2 e^2}{2} \sum_{i=1}^{\infty} (\alpha_i - x^2) I_i, \quad (5)$$

where $I_i = m_i/R_{in}$. If the ion placement is completely random, $\alpha_i = x^2$ for any i , $|\Delta_{\mathbf{k}}^+|^2 = Nx(1-x)$ throughout \mathbf{B}_1 , whereas $U_{\text{corr}} = 0$.

Static displacements of ions ($\ll a_i$) from the lattice nodes under the action of local forces not completely compensated due to lack of symmetry, may be expected to give rise to an energy contribution, U_{shft} , of the same order of magnitude as U_{corr} . After some algebra, it can be shown that to the lowest, $(\delta Z)^2$, order

$$U_{\text{shft}} = -\frac{(Z_2 - Z_1)^2 e^2}{2} [x(1-x) T_0 + \sum_{i=1}^{\infty} (\alpha_i - x^2) T_i]. \quad (6)$$

In this case,

$$T_i = \int_{\mathbf{B}_1} \frac{d\mathbf{k}}{(2\pi)^3 n_i} \sum_{s=1,2,3} \frac{|\mathbf{e}_{\mathbf{k}s} \cdot \mathbf{b}_{\mathbf{k}}|^2}{\lambda_{\mathbf{k}s}} \sum_{\mathbf{R}_{in}} \cos(\mathbf{k}\mathbf{R}_{in}) \quad (7)$$

at $i > 0$. T_0 has 1 in place of $\sum_{\mathbf{R}_{in}}$, whereas $\lambda_{\mathbf{k}s}$ are eigennumbers of a real symmetric 3×3 matrix $D_{\mathbf{k}\alpha\beta}$, and $\mathbf{e}_{\mathbf{k}s}$ are its three respective mutually orthogonal unit eigenvectors. Finally,

$$D_{\mathbf{k}\alpha\beta} = \sum_{\mathbf{R} \neq 0} (e^{i\mathbf{k}\mathbf{R}} - 1) g_{\alpha\beta}(\mathbf{R}) + n_i \int d\mathbf{r} g_{\alpha\beta}(\mathbf{r}), \quad (8)$$

$$\mathbf{b}_{\mathbf{k}} = - \sum_{\mathbf{R} \neq 0} e^{i\mathbf{k}\mathbf{R}} \mathbf{h}(\mathbf{R}), \quad (9)$$

where $g_{\alpha\beta}(\mathbf{r}) \equiv \delta_{\alpha\beta}/r^3 - 3r_{\alpha}r_{\beta}/r^5$ and $\mathbf{h}(\mathbf{r}) \equiv \mathbf{r}/r^3$. Practical expressions for the matrix $D_{\mathbf{k}\alpha\beta}$ and the vector $\mathbf{b}_{\mathbf{k}}$ can be obtained with the standard Ewald method. At low k , $\mathbf{b}_{\mathbf{k}} \approx 4\pi i n_i \mathbf{k}/k^2$.

We have calculated the integrals T_0 - T_8 on a dense grid of wavevectors in \mathbf{B}_1 and the results are given in Table I. Their inaccuracy can be estimated as ± 1 in the last digit. The degree of compensation between seemingly unrelated T_i and I_i is quite remarkable. U_{shft} , unlike

U_{corr} , is non-zero for a completely disordered binary mixture. Its electrostatic energy thus is $U_{\text{rnd}} = \langle U \rangle + U_{\text{shft}} = -e^2[\zeta\langle Z \rangle^2/a_i + 0.5T_0(Z_2 - Z_1)^2x(1-x)]$ (cf. Fig. 1).

For structural studies, one also requires residual entropy of the static lattice, i.e. the entropy which remains in the crystal mixture at zero temperature. For a completely disordered binary solid, the results is

$$S_{\text{mix}} = -Nx \ln x - N(1-x) \ln(1-x). \quad (10)$$

Ref. [13] used instead a slightly different quantity

$$S_{\text{mix}Z} = S_{\text{mix}} + N(\ln \langle Z \rangle - \langle \ln Z \rangle), \quad (11)$$

which we shall also utilize further, however, as discussed in [25], the choice of $S_{\text{mix}Z}$ was not convincingly justified. On the other hand, the residual entropy of a perfectly ordered crystal mixture, such as the CsCl system, is 0. It is then natural to expect that a crystal mixture with the short-range order considered in the present work would have a residual entropy intermediate between 0 and S_{mix} . We adopt an entropy estimate based on the idea of [24]. The details are provided in the Appendix.

Random C/O mixture – Let us apply the above theory to a dense C/O mixture. We shall plot energies and Helmholtz free energies with the linear mixing electrostatic energy, $-\zeta\langle Z^{5/3} \rangle e^2/a_e$, subtracted, and in units of $U_1 \equiv Z_1^{5/3} e^2/a_e$, where $a_e = (4\pi n_e/3)^{-1/3}$. Curves, describing the solid, contain nothing other than the electrostatic energies and residual entropies.

In the liquid, the free energies are given by the linear mixing rule based on the classic fit [26] plus the correction [27] and minus thermal free energies of the solid state given by the linear mixing rule and comprised of classic harmonic terms (including the average phonon frequency logarithm) and classic anharmonic terms of the first three orders [28]. Since these contributions are independent of or linear in x , their subtraction from the liquid quantities (instead of addition to the solid quantities) does not alter the outcome of the double tangent construction. At $x = 0$, the liquid free energy thus defined becomes zero at temperature $T = T_{1m}$, where $T_{1m} \equiv U_1/\Gamma_{1m}$ and $\Gamma_{1m} = 175.719$. In Fig. 1, we plot the liquid free energy (minus the solid terms) at $T = T_{1m}$ by the black dashed curve.

Open symbols in Fig. 1 show numerical calculations of corrections to linear-mixing energies of the solid state [13] with circles representing the “minimum” Monte Carlo (MC) energies, and squares corresponding to the fully-ordered configurations, CsCl and 4{fcc}. Dotted and thick solid curves show the fit proposed in [13] and U_{rnd} , respectively. The latter provides a better fit to the open circles at $x = 0.25, 0.5$, and 0.75 but a worse fit at $x = 0.01157$ (cf. inset). Such an agreement between first-principle and semi-analytic studies is extremely valuable. While the results of the former are reliable, they provide little insight into the physical processes, occurring in the system. By contrast, the results of the latter have clear physical meaning.

Dot-dashed and solid curves depict Helmholtz free energies. They are obtained from the dotted and thick

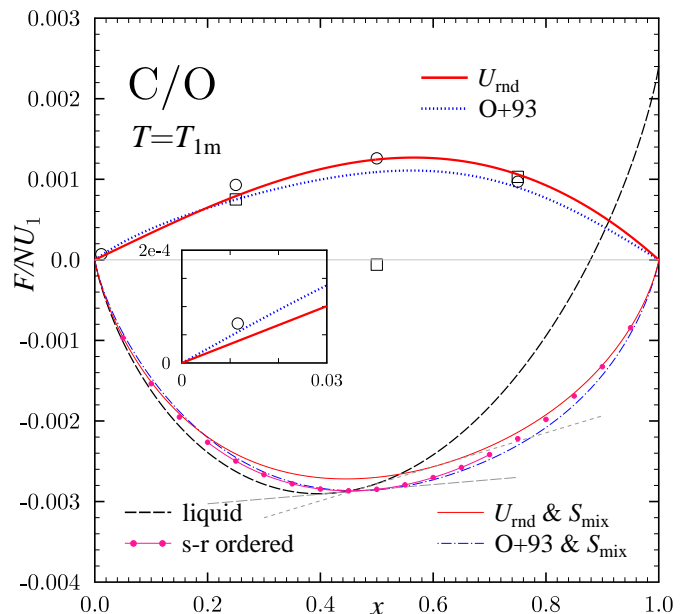


FIG. 1: Various energy and free energy models for C/O mixture at $T = T_{1m}$. Corrections to linear-mixing energies of the crystal reported in Ref. [13]: “minimum” MC energies (open circles), energies of fully-ordered configurations (squares), fit (dense dotted). Thick solid curve shows U_{rnd} . Helmholtz free energies: based on the fit [13] (dot-dashed), $U_{\text{rnd}} - TS_{\text{mix}}/N$ (solid), minimized with respect to the short-range order parameters (filled dots with a thin solid line, going through them), of the liquid (black dashes). Straight grey dashes illustrate double tangents.

solid curves (of the same color) by subtracting TS_{mix}/N . Straight short-dashed grey line is the double-tangent construction for the random-solid model at $T = T_{1m}$.

Let us note in passing that the horizontal line $F = 0$ in Fig. 1 represents the free energy of a mechanical mixture of pure C and O crystallites, whereas the open squares represent the free energies of the respective ordered mixtures. Both types of systems have zero residual entropies.

Phase diagrams based on the free energy models, depicted in Fig. 1, are plotted in Fig. 2 by dot-dashed and solid lines for fit [13] and disordered crystal model, respectively. In the case of fit [13], by dashes, we also show the phase diagram for which the solid free energy is obtained from the energy by subtracting $TS_{\text{mix}Z}/N$. The diagrams, originating from fit [13], are the same as those obtained in [29], and, in the case of $S_{\text{mix}Z}$ usage, the liquid-solid “banana” coincides with that of Ref. [14].

Short-range ordered C/O mixture – The question that naturally arises is whether a short-range order in a mixture could result in a thermodynamically preferred state. To see this, one has to minimize the free energy with respect to the order parameters. The latter must satisfy constraint (4), inequality above it, and the condition $|\Delta_{\mathbf{k}}^+|^2 \geq 0$ throughout B_1 . In this work, we do not study oscillations of ions around their equilibrium positions. In

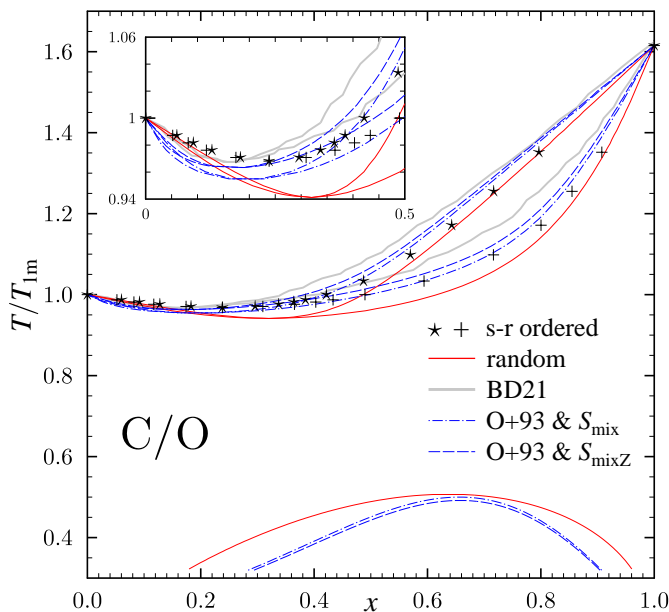


FIG. 2: C/O phase diagram for a short-range ordered crystal (symbols), fully disordered crystal (solid), based on simulations [18] (thick solid grey), based on the energy model [13] with the residual entropy equal to S_{mix} (dot-dashed) or S_{mixZ} (dashed).

principle, another constraint should be that the frequencies of these oscillations are real at any \mathbf{k} in B_1 .

We have performed such minimization with 8 order parameters at various x and Γ values ($\Gamma \equiv U_1/T$). In the process, we have checked the condition $|\Delta_{\mathbf{k}}^+|^2 \geq 0$ at $\sim 10^5$ wavevectors in the primitive part of B_1 , including 600 points on its 6 edges (including vertices), 4000 random points on its 4 faces, and $\sim 10^5$ random points in the inner region. Free energies minimized with 7 or 8 order parameters differed very little, by 1-2 in the fourth significant digit. Minimization with 6 order parameters was slightly worse at the highest considered $\Gamma \sim 700$ -800.

In Fig. 3, we plot relative deviations from x^2 of the order parameters, realizing free energy minima, vs. Γ at $x = 0.5$. Squares and crosses depict odd and even neighbor shells, respectively. The lowest Γ point is Γ_{1m} .

In Fig. 1, by filled dots, we show minimized crystal free energies at $T = T_{1m}$. A thin solid line, going through the dots, is a segment of a natural cubic spline. Straight long-dashed grey line is a double tangent between the spline and the liquid free energy.

By repeating this construction at various values of Γ from 130 to 181.5, we have mapped out the phase diagram of C/O liquid crystallization into a short-range ordered solid. It is shown by symbols in Fig. 2, where stars and pluses represent liquidus and solidus, respectively. We note that the free energies of the short-range ordered solid tend to free energies of the fully disordered solid at $x, 1-x \ll 1$. As a result, symbols approach the solid curves in Fig. 2 at low and high x .

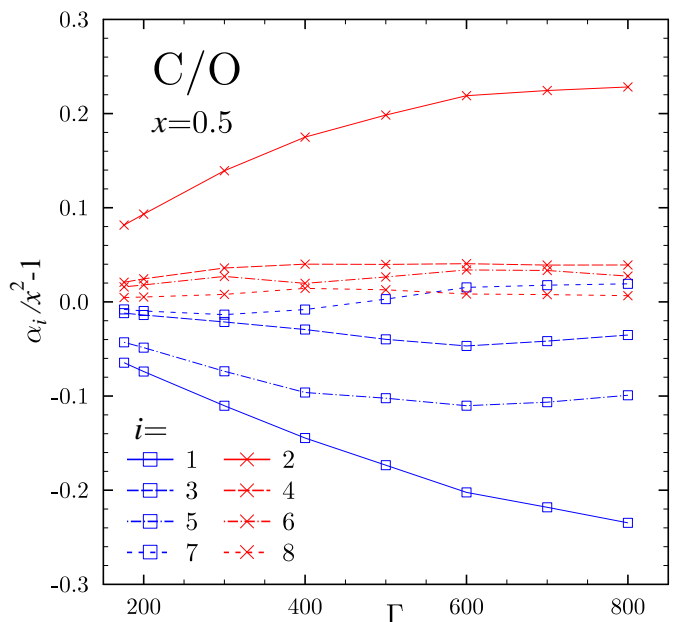


FIG. 3: Odd (squares) and even (crosses) order parameters at free energy minimum.

The models of fully disordered and short-range ordered solids reported in this work are the first models of crystallized mixtures, not involving ab initio simulations, which predict azeotropic C/O phase diagram, thereby explaining the diagram shape in a transparent way. Thick solid grey curves in Fig. 2 show currently the most advanced first-principle based C/O phase diagram [18]. We observe a decent agreement of our symbols with this diagram especially at $x \lesssim 0.2$, indicating a preference for the short-range order. The agreement worsens at higher x , and, at this point, it is worth listing certain shortcomings of our present approach, which may be responsible for the discrepancy. Firstly, our energy expression does not contain cubic and higher-order terms in δZ , which would otherwise contribute to U_{shft} . Secondly, a more self-consistent expression for the residual entropy is desired. Thirdly, the treatment of harmonic and anharmonic ion vibrations around their equilibrium positions in the lattice is presently limited to the linear mixing rule and can be improved. Such future improvement should also allow one to exclude phonon-unstable configurations from the free energy minimization procedure.

Equilibrium C/O crystal structure – Fig. 3 indicates that the order parameters at thermal equilibrium evolve with temperature. This means that whatever structure is formed upon crystallization, it ceases to be a preferred state as soon as the temperature drops. Free energy of this structure at a lower temperature can be obtained from its free energy at crystallization by rescaling the entropy term with the ratio of new and crystallization temperatures. In Fig. 4, we show by crosses the free energy difference between such rescaled free energy and the true equilibrium free energy at low T and four val-

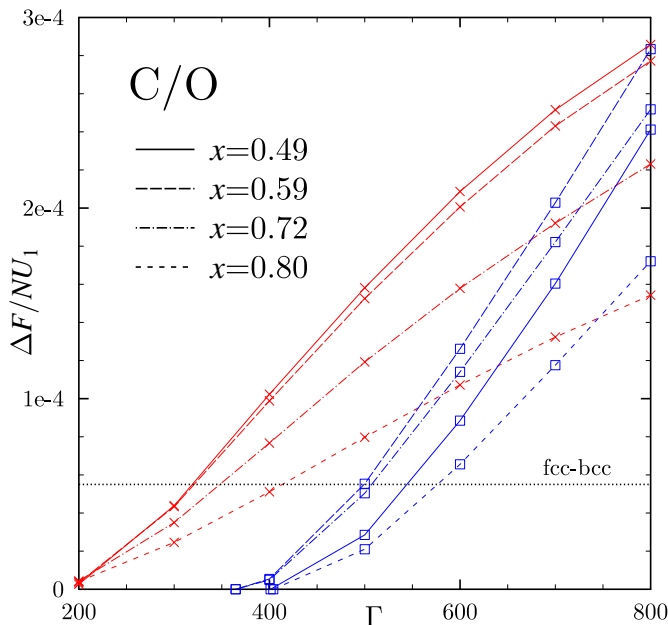


FIG. 4: Free energy gain from short-range ordering (crosses), exsolution (squares), fcc to bcc structural transition (dotted).

ues of $x \approx 0.49, 0.59, 0.72,$ and 0.80 , corresponding to crystallization at $\Gamma = \Gamma_{1m}, 170, 160,$ and 150 , respectively. For comparison, the energy difference between one-component fcc and bcc crystals is shown by dots.

This picture of evolving equilibrium structure of a crystal mixture is different from the one implied by the lower portion of Fig. 2. In the latter, it is assumed that the mixture below crystallization has a fixed microstructure but, at some critical T and x , its free energy becomes larger than the free energy of a mechanical sum of two such mixtures, with lower and higher Z_2 fractions. This signifies the exsolution onset and the appearance of the miscibility gap bounded by the solvus curve [29]. The free energy gain, resulting from the exsolution process (for the dashed solvus in Fig. 2), is also shown in Fig. 4 by squares for the same values of x . It is typically smaller than the gain from crystal short-range reordering and, unlike the latter, it becomes nonzero not at the crystallization temperature but at the solvus temperature.

It is hard to say what the fate of a crystal mixture, having a nonequilibrium structure, is in actual degenerate stars. It is a question for kinetics. We can assert though that if any kind of restructuring does occur with temperature decrease, it will be accompanied by thermal energy release and an effect on stellar cooling similar to that studied in [25, 30].

Conclusion – We have proposed a new method of analysis of a crystallized binary mixture of atomic nuclei on neutralizing electron background which serves as a model of matter in the inner layers of degenerate stars. The method includes (i) introduction of short-range order pa-

rameters to specify average mutual arrangement of nuclei of two sorts; (ii) exact expression for the electrostatic energy of a short-range ordered mixture, assuming all ions are located precisely at the lattice nodes; (iii) lowest order correction to the electrostatic energy due to static ion displacements from their nodes; (iv) estimate of the mixture residual entropy with account of partial ordering; (v) minimization of the free energy with respect to the order parameters to determine the equilibrium state. This is the first application of the short-range ordering idea to crystal mixtures of atomic nuclei and the first qualitative and quantitative description of the microstructure of these systems.

Being applied to a C/O mixture, the method allows one to (i) explain the results of simulations [13] with regard to “minimum” MC crystal mixture energy; (ii) prove that C and O positions on a lattice are not random but are short-range ordered; (iii) find the order parameter dependence on temperature; (iv) obtain C/O phase diagram in a decent agreement with the diagram [18], the most recent one based on first-principle simulations, especially in the region $x \lesssim 0.2$, where it is hard to achieve good resolution (cf. [15]); (v) reappraise the situation below crystallization temperature, where instead of an abrupt transition to a state with a miscibility gap, the equilibrium state is predicted to have a continuously evolving structure. In summary, this is the first model, not relying on ab initio simulations of crystallized mixtures, which predicts azeotropic C/O phase diagram shape. By proposing, for the first time, a plausible ordering in the system, the diagram is brought into a reasonable agreement with that obtained in the most recent first-principle study.

In the future, the mixture microstructure obtained here can be a starting point for more detailed studies of ion thermodynamics as well as for calculations of electron-ion scattering rates, which determine kinetic coefficients. The formalism can be readily extended to mixtures of more than two ion types which, among other applications, would allow one to verify independently ^{22}Ne -depletion and buoyancy of crystals in C/O/ ^{22}Ne mixtures [1, 2] which is presently invoked for explanation of both multi-Gyr WD cooling delays [3] and their strong magnetic field generation [31].

Acknowledgment – The author is grateful to A. A. Kozhberov with whom the definition of $\delta Z(\mathbf{R})$ and its Fourier transform was discussed. This work was supported by Russian Science Foundation, grant 24-12-00320.

Appendix

Residual entropy – Let us select a vector \mathbf{R}_{in} from an ion to its i th order neighbor. There are N such vectors in the lattice, Nx of which originate from Z_2 while $N(1-x)$ from Z_1 . Of the Nx vectors, originating from Z_2 , a fraction α_i/x must point to another Z_2 . Therefore, there are in total $N\alpha_i [Z_2Z_2]$ \mathbf{R}_{in} -links and $N(x-\alpha_i) [Z_2Z_1]$

\mathbf{R}_{in} -links. Thus, there are also $N(x - \alpha_i)$ $[Z_2 Z_1]$ links, corresponding to the opposite vector $-\mathbf{R}_{in}$. And thus there are in total $N(x - \alpha_i)$ and $N(1 - 2x + \alpha_i)$ $[Z_1 Z_2]$ and $[Z_1 Z_1]$ \mathbf{R}_{in} -links, respectively.

We aim to express the entropy via these numbers of links, which guarantee that the order parameters have the desired values. Since the direct calculation is known to diverge [24], we shall consider the entropy decrement due to the difference between α_i and x^2 . If all $\alpha_i = x^2$, then the total entropy is of course S_{mix} .

The calculation is based on the number of ways N links can be split into 4 groups such that permutations within each group do not matter. Then the entropy decrement becomes

$$\Delta S(\mathbf{R}_{in}) = \ln \frac{H(\alpha_i)}{H(x^2)}, \quad (\text{A.1})$$

where

$$H(\alpha) = \frac{N!}{(N\alpha)! \{ [N(x - \alpha)]! \}^2 [N(1 - 2x + \alpha)]!}. \quad (\text{A.2})$$

Using Stirling's formula, we obtain

$$\begin{aligned} \frac{\Delta S(\mathbf{R}_{in})}{N} &= 2x \ln x + 2(1 - x) \ln(1 - x) \\ &- \alpha_i \ln \alpha_i - 2(x - \alpha_i) \ln(x - \alpha_i) \\ &- (1 - 2x + \alpha_i) \ln(1 - 2x + \alpha_i). \quad (\text{A.3}) \end{aligned}$$

Since there is nothing special about the vector \mathbf{R}_{in} , the total entropy decrement becomes

$$S - S_{\text{mix}} = \frac{1}{2} \sum_i m_i \Delta S(\mathbf{R}_{in}), \quad (\text{A.4})$$

where $1/2$ takes into account the fact that links, corresponding to \mathbf{R}_{in} and $-\mathbf{R}_{in}$ are the same.

Just like [24], we realize that there are interactions between links, corresponding to different vectors, which, presumably, will give rise to contributions to equation (A.4), containing higher powers of the order parameter. However, this problem is too complicated, and, for the time being, we treat different contributions as independent.

The entropy S given by equation (A.4) is not bounded from below and, in particular, if $\alpha_i = x$ is assumed for all i , which corresponds to separation of charges Z_1 and Z_2 and thus to zero entropy, equation (A.4) predicts $-\infty$. In our numerical work, we have implemented a check of the entropy sign and did not allow states with $S < 0$. However, this has not affected results reported in this paper because all configurations, realizing free energy minima, had residual entropies well above zero.

-
- [1] J. Isern, M. Hernanz, R. Mochkovitch, and E. García-Berro, *Astron. Astrophys.* **241**, L29 (1991)
- [2] S. Blouin, J. Daligault, and D. Saumon, *Astrophys. J. Lett.* **911**, L5 (2021).
- [3] A. Bédard, S. Blouin, and S. Cheng, *Nature* **627**, 286 (2024).
- [4] D.J. Stevenson, *Phys. Lett. A* **58**, 282 (1976).
- [5] J.P. Hansen, G.M. Torrie, and P. Vieillefosse, *Phys. Rev. A* **16**, 2153 (1977).
- [6] D.J. Stevenson, *J. Phys. Colloques* **41**, C2-61 (1980).
- [7] J.L. Barrat, J.P. Hansen, and R. Mochkovitch, *Astron. Astrophys.* **199**, L15 (1988).
- [8] S. Ichimaru, H. Iyetomi, and S. Ogata, *Astrophys. J.* **334**, L17 (1988).
- [9] L. Segretain and G. Chabrier, *Astron. Astrophys.* **271**, L13 (1993).
- [10] H.E. Dewitt, W.L. Slattery, and G. Chabrier, *Physica B* **228**, 21 (1996).
- [11] L. Segretain, *Astron. Astrophys.* **310**, 485 (1996).
- [12] H.E. Dewitt and W.L. Slattery, *Contrib. Plasm. Phys.* **43**, 279 (2003).
- [13] S. Ogata, H. Iyetomi, S. Ichimaru, and H.M. Van Horn, *Phys. Rev. E* **48**, 1344 (1993).
- [14] Z. Medin and A. Cumming, *Phys. Rev. E* **81**, 036107 (2010).
- [15] C.J. Horowitz, A.S. Schneider, and D.K. Berry, *Phys. Rev. Lett.* **104**, 231101 (2010).
- [16] J. Hughto, C.J. Horowitz, A.S. Schneider, Z. Medin, A. Cumming, and D.K. Berry, *Phys. Rev. E* **86**, 066413 (2012).
- [17] M.E. Caplan, C.J. Horowitz, and A. Cumming, *Astrophys. J. Lett.* **902**, L44 (2020).
- [18] S. Blouin and J. Daligault, *Phys. Rev. E* **103**, 043204 (2021).
- [19] S. Blouin and J. Daligault, *Astrophys. J.* **919**, 87 (2021).
- [20] M.E. Caplan, I.F. Freeman, C.J. Horowitz, A. Cumming, and E.P. Bellinger, *Astrophys. J. Lett.* **919**, L12 (2021).
- [21] M.E. Caplan, S. Blouin, and I.F. Freeman, *Astrophys. J.* **946**, 78 (2023).
- [22] A.A. Kozhberov, *Astron. Lett.* **50**, 523 (2024).
- [23] A.A. Kozhberov, *Phys. Rev. E* **110**, 045206 (2024).
- [24] J.M. Cowley, *Phys. Rev.* **138**, A1384 (1965).
- [25] D.A. Baiko, *Mon. Not. Roy. Astron. Soc.* **522**, L26 (2023).
- [26] A.Y. Potekhin and G. Chabrier, *Phys. Rev. E* **62**, 8554 (2000).
- [27] A.Y. Potekhin, G. Chabrier, A.I. Chugunov, H.E. Dewitt, and F.J. Rogers, *Phys. Rev. E* **80**, 047401 (2009).
- [28] D.A. Baiko and A.I. Chugunov, *Mon. Not. Roy. Astron. Soc.* **510**, 2628 (2022).
- [29] D.A. Baiko, *Mon. Not. Roy. Astron. Soc.* **517**, 3962 (2022).
- [30] M. Camisassa, D.A. Baiko, S. Torres, and A. Rebassamansergas, *Astron. Astrophys.* **683**, A101 (2024).
- [31] A.F. Lanza, N.Z. Rui, J. Farihi, J.D. Landstreet, and S. Bagnulo, *Astron. Astrophys.* **689**, A233 (2024).